processes

MDPI

Article

Phase Equilibrium of the Quaternary System LiBr-Li_2SO_4-KBr-K_2SO_4-H_2O at 308.15 K

Bin Li [1,2,3], Xinjun Jing [4] and Junsheng Yuan [1,2,3,*]

[1] School of Chemical Engineering and Technology, Hebei University of Technology, Tianjin 300130, China; libin940916@163.com
[2] Engineering Research Center of Seawater Utilization of Ministry of Education, Tianjin 300130, China
[3] Hebei Collaborative Innovation Center of Modern Marine Chemical Technology, Tianjin 300130, China
[4] Hebei Datang International Wangtan Power Generation Co., Ltd., Tangshan 063611, China; jingxj961015@163.com
* Correspondence: jsyuan2012@126.com

Abstract: The phase equilibria of the reciprocal quaternary system LiBr-Li_2SO_4-KBr-K_2SO_4-H_2O and its ternary sub-systems LiBr-Li_2SO_4-H_2O and KBr-K_2SO_4-H_2O at 308.15 K were studied using the isothermal dissolution equilibrium method. Then, the solubility data of the equilibrium solutions were collected, and the phase diagrams were plotted. The phase diagrams of the ternary sub-systems at 308.15 K were compared with those at other temperatures. This study found that the phase diagram of the LiBr-Li_2SO_4-H_2O system at 308.15 K consisted of an invariant point, two solid-phase crystallization regions of $Li_2SO_4 \cdot H_2O$ and $LiBr \cdot 2H_2O$, and their corresponding solubility curves. The system generated two hydrated salts, which belonged to the hydrate type I phase diagram. The phase diagram of the KBr-K_2SO_4-H_2O system at 308.15 K consisted of an invariant point, two univariant solubility curves, and two solid-phase crystallization regions of KBr and K_2SO_4, and no solid solution and double salts were formed. Thus, it belonged to a simple co-saturation type phase diagram. In the LiBr-Li_2SO_4-KBr-K_2SO_4-H_2O system, $K_2SO_4 \cdot Li_2SO_4$ double salt formed at 308.15 K, and the phase diagram consisted of three invariant points, five crystallization regions, and seven univariant solubility curves.

Keywords: lithium bromide; potassium bromide; lithium sulfate; potassium sulfate; phase equilibrium

Citation: Li, B.; Jing, X.; Yuan, J. Phase Equilibrium of the Quaternary System LiBr-Li_2SO_4-KBr-K_2SO_4-H_2O at 308.15 K. *Processes* **2022**, *10*, 823. https://doi.org/10.3390/pr10050823

Academic Editors: Lutz Böhm, Matthias Kraume and Michael Schlüter

Received: 31 March 2022
Accepted: 20 April 2022
Published: 21 April 2022

1. Introduction

Lithium and its compounds have been widely used in aerospace, battery materials, ceramic glass, aluminum electrolysis, medicine, and other fields [1]. Lithium resources mainly exist in salt-lake brine and ore, among which lithium reserves in brine account for about 70–80% of total lithium resources [2,3]. To meet the increasing demand for lithium resources, the development and extraction of lithium from brine are needed [4]. Global lithium resources are mainly distributed in South American countries, Australia, and China [5]. The Sichuan Basin in China contains rich brine reserves and has a long mining history. Before 1949, salt mines were mined mainly for human consumption, thus only sodium chloride was extracted, and some useful resources, such as Li^+, K^+, Br^-, B^{3+}, Sr^{2+}, Rb^+, Cs^+, I^-, have been underutilized [6]. Since the beginning of the 21st century, due to the rapid development of new energy vehicles, the demand for lithium resources has grown, which drives the research on lithium extraction from brine [7].

Because brine is a complex electrolyte system, its comprehensive utilization depends on the guidance of the water–salt system phase diagram. In recent years, numerous studies have been conducted around the brine system in the Sichuan Basin [8], and the results indicated that the LiBr-KBr-H_2O system at 273.15 K [9], 288.15 K [10], 298.15 K [11], 308.15 K [9] and 323.15 K [12] showed simple co-saturation phase diagrams, confirming that double salt $K_2SO_4 \cdot Li_2SO_4$ will form in the Li_2SO_4-K_2SO_4-H_2O system at these temperatures [13–16].

In the LiBr-Li_2SO_4-H_2O system, the corresponding solid phases of the saturation point at 298.15 K were $Li_2SO_4 \cdot H_2O$ and $LiBr \cdot 2H_2O$ [17]. The KBr-K_2SO_4-H_2O system at multiple temperatures [18–20] all showed simple co-saturation type phase diagrams.

To realize the utilization of underground brine in the Sichuan Basin, the phase diagram of LiBr-Li_2SO_4-KBr-K_2SO_4-H_2O and its sub-systems (LiBr-Li_2SO_4-H_2O, KBr-K_2SO_4-H_2O) were studied at 308.15 K and 100.5 kPa in this work. Many studies have been conducted on related quaternary systems, such as the LiBr-Li_2SO_4-NaBr-Na_2SO_4-H_2O [21], LiCl-Li_2SO_4-KCl-K_2SO_4-H_2O [22,23], NaBr-Na_2SO_4-KBr-K_2SO_4-H_2O [24–26], and NaCl-Na_2SO_4-KCl-K_2SO_4-H_2O systems [27]. On the basis of these research results, the phase diagrams of these quaternary systems were compared, and the phase equilibrium characteristics of these quaternary systems were summarized.

2. Experimental Materials and Methods

2.1. Experimental Reagents and Instruments

Table 1 lists the main experimental reagents. The pH of the distilled water in the experiment was 6.65 and the conductivity was less than 0.8×10^{-4} S/m.

Table 1. Chemical Reagents.

Chemical Reagent	CAS Reg. No.	Mass Fraction Purity	Supplier
LiBr	7550-35-8	≥99.90%	Aladdin Industrial Corporation
Li_2SO_4	10377-48-7	≥99.99%	Aladdin Industrial Corporation
KBr	7758-02-3	≥99.95%	Aladdin Industrial Corporation
K_2SO_4	7778-80-5	≥99.99%	Aladdin Industrial Corporation

The main instruments used in the experiment are shown in Table 2. The composition of the solid phase in equilibrium was determined by X-ray diffraction. The magnetic stirring thermostatic bath was used to ensure the constant stirring speed and temperature of the solution during the reaction process.

Table 2. Chemical Instruments.

Instrument Name	Type	Accuracy of Measurement	Supplier
X-ray diffraction	DSFOCUS	-	Da Vinci type, Brucker AXS, Germany
A magnetic stirring thermostatic bath	HXC-500-8A	±0.05 K	Changzhou Langyue Instrument Manufacturing Co., Ltd., China
Electric blast drying oven	101-1ABS	±1 K	Beijing Yongguangming Medical Instrument Factory, China
Electronic balance	FA2204B	±0.0001 g	Shanghai Youke Instrument Co., Ltd., China

2.2. Experimental Methods

The solubility of each system in this work was obtained by the isothermal dissolution method. First, the solubility of KBr, K_2SO_4, LiBr, and Li_2SO_4 at 308.15 K were determined and verified. Subsequently, additional salt was introduced into the saturated binary system solution gradually, and the solubilities of the ternary systems were obtained after they reached the dissolution equilibrium. Finally, a third salt was gradually introduced to the invariant-point solution of the ternary sub-system to obtain the phase solubility of the LiBr-Li_2SO_4-KBr-K_2SO_4-H_2O system. During experimentation, the prepared solution was stirred for 12 h and allowed to stand for 10 h to obtain the supernatant. Then, the liquid phase composition of the supernatant was determined. These experimental procedures

were repeated until the liquid phase composition of the solution showed no more changes, indicating that the system reached equilibrium. The experimental results show that the LiBr-Li_2SO_4-KBr-K_2SO_4-H_2O system reached equilibrium after 6–9 days at 308.15 K. This equilibrium time was consistent with the literature [19,21,22].

In the quaternary system calculations, the Jänecke index (J) values of each ion, and H_2O were used, and the calculation methods are shown in Equations (1)–(6). In this paper, the proportion of different ions in the saturated solution was expressed by mass fraction (w).

$$A = \frac{w(Li^+)}{13.882} + \frac{w(K^+)}{78.197} + \frac{w(Br^-)}{159.808} + \frac{w(SO_4^{2-})}{96.063} \quad (1)$$

$$J\left(Li_2^{2+}\right) = \frac{w(Li^+)}{A \times 13.882} \times 100 \times 2 \quad (2)$$

$$J\left(K_2^{2+}\right) = \frac{w(K^+)}{A \times 78.197} \times 100 \times 2 \quad (3)$$

$$J\left(Br_2^{2-}\right) = \frac{w(Br^-)}{A \times 159.808} \times 100 \times 2 \quad (4)$$

$$J\left(SO_4^{2-}\right) = \frac{w(SO_4^{2-})}{A \times 96.063} \times 100 \times 2 \quad (5)$$

$$J(H_2O) = \frac{w(H_2O)}{A \times 18.02} \times 100 \times 2 \quad (6)$$

2.3. Analysis Methods

The chemical analysis method for each ion in this work was as follows. The concentration of Li^+ was obtained according to the atomic absorption assisted subtraction method (uncertainty within ± 0.005), the concentration of K^+ content was measured by the atomic absorption method (uncertainty within ± 0.005), the concentration of Br^- was determined according to the silver nitrate titration method (uncertainty within ± 0.005), and the concentration of SO_4^{2-} was determined by the sulfate gravimetric method (uncertainty within ± 0.005). The solid phase composition at equilibrium was measured by the wet-residue method and X-ray diffraction crystallography.

3. Results and Discussion

3.1. Phase Equilibrium of the LiBr-Li_2SO_4-H_2O System

Table 3 shows the solubility data in the LiBr-Li_2SO_4-H_2O system at 308.15 K. The XRD characterization patterns of invariant point E_1 are shown in Figure 1. According to Table 3, the phase diagram of the LiBr-Li_2SO_4-H_2O system at 308.15 K was drawn (Figure 2a), and Figure 2b shows a partially enlarged view near invariant point E_1.

A_1 and B_1 represented the pure solid phase points of $Li_2SO_4 \cdot H_2O$ and $LiBr \cdot 2H_2O$ (Figure 2), respectively, C_1 and D_1 were the saturation points of Li_2SO_4-H_2O and LiBr-H_2O, respectively, E_1 denoted the invariant point of the system, and the liquid phase compositions at this point were w(LiBr) = 63.21%, w(Li_2SO_4) = 0.01%, and w(H_2O) = 36.78%. The equilibrium solid phases at this point were $Li_2SO_4 \cdot H_2O$ and $LiBr \cdot 2H_2O$. Curve C_1E_1 indicated the solubility curve of $Li_2SO_4 \cdot H_2O$, and curve D_1E_1 corresponded to the solubility curve of $LiBr \cdot 2H_2O$. Fields $A_1C_1E_1$ and $B_1D_1E_1$ denoted the crystallization regions of $Li_2SO_4 \cdot H_2O$, and $LiBr \cdot 2H_2O$, respectively. Fields $A_1E_1B_1$ was the crystallization region of $Li_2SO_4 \cdot H_2O$ and $LiBr \cdot 2H_2O$.

The phase diagram consisted of two solid crystalline regions $Li_2SO_4 \cdot H_2O$ and $LiBr \cdot 2H_2O$, two solubility curves C_1E_1 and D_1E_1, and one saturation point E_1. The system generated two hydrated salts; therefore, its phase diagram belonged to hydrate type I. The C_1E_1 curve in Figure 2a indicated that the mass percentage of Li_2SO_4 decreased sharply with LiBr addition. When the mass percentage of LiBr was 39.61%, the content of Li_2SO_4 dropped below 1%, and the crystallization region of $LiBr \cdot 2H_2O$ occupied a very small area in the

phase diagram. This shows that LiBr had a strong salting-out effect on $Li_2SO_4 \cdot H_2O$, making it easier to separate from the solution.

The phase equilibrium data of the LiBr-Li_2SO_4-H_2O system at the co-saturation points of 298.15 K and 308.15 K are shown in Table 4. The phase diagrams of the system at these two temperatures are shown in Figure 3. By comparison, we found that the number of saturation points, solubility curves, and crystallization zones of the system were the same at these two temperatures. The equilibrium solid phases corresponding to the saturation point were $LiBr \cdot 2H_2O$ and $Li_2SO_4 \cdot 2H_2O$. The difference was that when the temperature increased by 10 K, the mass fraction (w) of Li_2SO_4 in the system decreased from 25.78% to 25.35%, while the mass fraction (w) of LiBr in the system increased from 62.16% to 63.93%. Meanwhile, the crystallization zone of $Li_2SO_4 \cdot 2H_2O$ increased while that of $LiBr \cdot 2H_2O$ decreased. Based on this observation, we could fabricate an $LiBr \cdot 2H_2O$ crystal by lowering the temperature.

Table 3. Solubility of LiBr-Li_2SO_4-H_2O at 308.15 K and 100.5 kPa [a].

No.	Composition of Liquid Phase/w (%)		Wet Solid Phase/w (%)		Solid Phase
	LiBr	Li_2SO_4	LiBr	Li_2SO_4	
1, C_1	0.00	25.35	-	-	Ls1
2	4.63	21.10	1.72	63.04	Ls1
3	11.08	15.27	5.60	50.93	Ls1
4	21.32	9.07	9.99	49.87	Ls1
5	27.15	6.03	8.68	60.49	Ls1
6	33.31	2.71	12.35	54.77	Ls1
7	39.61	0.63	11.82	60.57	Ls1
8	42.48	0.18	9.99	66.06	Ls1
9	45.17	0.10	14.90	57.54	Ls1
10	49.88	0.05	11.82	65.73	Ls1
11	52.52	0.03	15.90	60.08	Ls1
12	56.54	0.02	14.18	64.26	Ls1
13, E_1	63.21	0.01	54.77	17.13	Ls1 + Lb2
14, D_1	63.93	0.00	-	-	Lb2

[a] Standard uncertainties: u(T) = 0.05 K; u(P) = 2 kPa; u(mass fraction) = 0.03; Ls1, $Li_2SO_4 \cdot H_2O$, Lb2, $LiBr \cdot 2H_2O$.

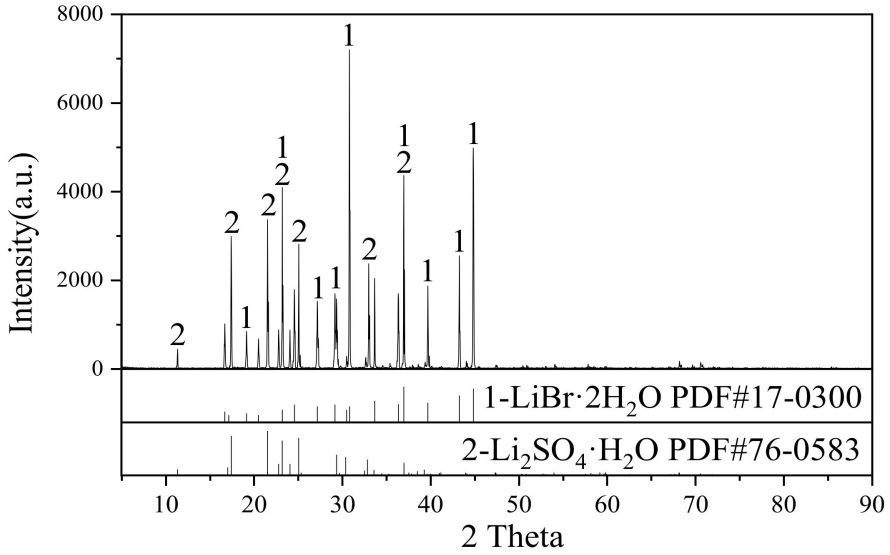

Figure 1. XRD spectrogram of the saturation point E_1 of LiBr-Li_2SO_4-H_2O at 308.15 K.

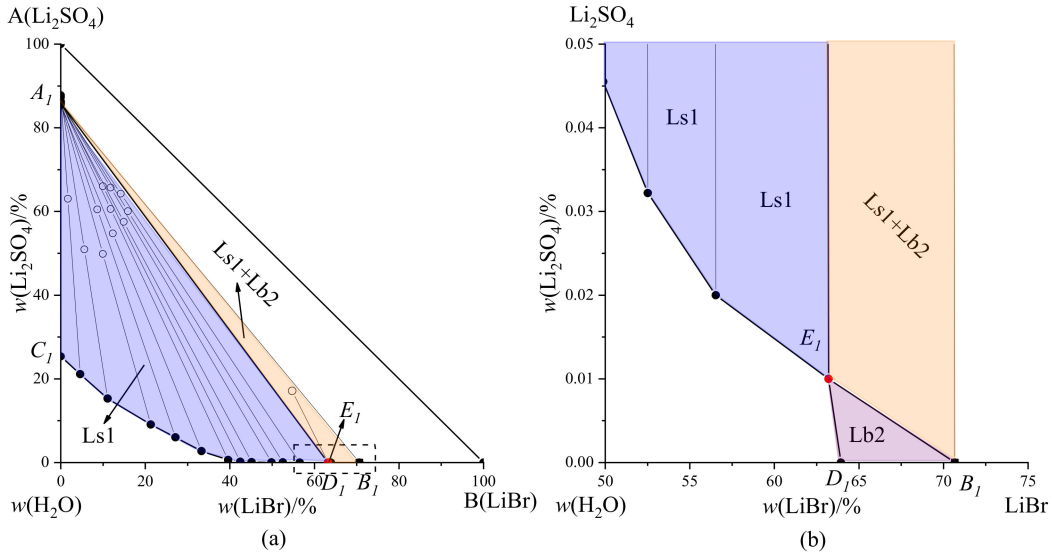

Figure 2. (**a**) Phase diagram of LiBr-Li_2SO_4-H_2O at 308.15 K and (**b**) enlarged view of point E_1. ●, the equilibrium liquid-phase composition point; ○, wet residue composition point.

Table 4. Solubilities of salts at the invariant points. In ternary system LiBr-Li_2SO_4-H_2O at 298.15 K and 308.15 K.

Temperature/K	Refs	Composition of Liquid Phase/*w* (%)		Solid Phase
		LiBr	Li_2SO_4	
298.15	[21]	62.16	0.00	$LiBr·2H_2O$
		61.27	0.07	$Li_2SO_4·H_2O$ + $LiBr·2H_2O$
		0.00	25.78	$Li_2SO_4·H_2O$
308.15	this work	63.93	0.00	$LiBr·2H_2O$
		63.22	0.01	$Li_2SO_4·H_2O$ + $LiBr·2H_2O$
		0.00	25.35	$Li_2SO_4·H_2O$

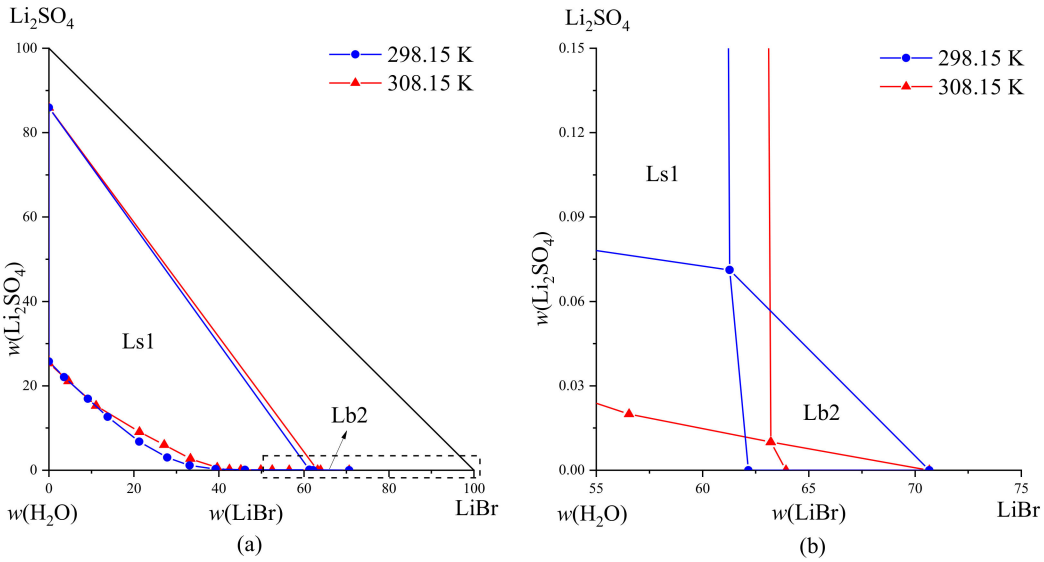

Figure 3. (**a**) Equilibrium phase diagram of ternary system LiBr-Li_2SO_4-H_2O at different temperatures; (**b**) partial enlargement. Ls1, $Li_2SO_4·H_2O$; Lb2, $LiBr·2H_2O$.

3.2. Phase Equilibrium of the KBr-K_2SO_4-H_2O System

Table 5 shows the solubility data of the KBr-K_2SO_4-H_2O system at 308.15 K, where the solid phase was analyzed by XRD characterization. The results indicated that the equilibrium solid phases of sample no. 13 were K_2SO_4 and KBr (Figure 4). The phase diagram (Figure 5a) was plotted based on the solubility data, and Figure 5b presents a partially enlarged view near invariant point E_2.

Points A_2 and B_2 corresponded to solid phases K_2SO_4 and KBr, respectively, while point C_2 and D_2 was the saturation point of K_2SO_4-H_2O and KBr-H_2O (Figure 5a), where $w(K_2SO_4)$ was 12.05% and w(KBr) was 42.21%. In addition, the liquid phase composition was w(KBr) = 41.77%, $w(K_2SO_4)$ = 0.59%, and $w(H_2O)$ = 57.64% in saturated point E_2, and the equilibrium solid phases at this point were KBr and K_2SO_4.

The C_2E_2 curve was the solubility curve of K_2SO_4, where $A_2E_2C_2$ denoted the crystallization region of K_2SO_4. The solid phase corresponding to the solubility curve D_2E_2 in the partially enlarged view shown in Figure 5b was KBr, and $B_2D_2E_2$ was the crystallization region of KBr. As shown in Figure 5a, the region occupied by $A_2E_2C_2$ in the triangle was considerably larger than $B_2D_2E_2$, indicating that the crystallization region of KBr in this system was smaller than that of K_2SO_4, and had a strong salting-out effect on K_2SO_4. This system did not generate a solid solution or hydrated salts at 308.15 K; thus, it consisted of a simple phase diagram.

Table 6 lists the phase equilibrium data of the co-saturation points of the KBr-K_2SO_4-H_2O system at different temperatures. A comparison of phase diagrams is shown in Figure 6. The results show that the phase diagrams had the same characteristics at these three different temperatures, and the equilibrium solid phases corresponding to the saturation point were KBr and K_2SO_4. The mass percentage of K_2SO_4 in the K_2SO_4-H_2O system increased from 6.78% to 19.4%, and the mass percentage of KBr in the KBr-H_2O system increased from 34.11% to 50.98% when the temperature increased by 100 K. By analyzing the data of the saturation points at different temperatures, we found that KBr had a strong salting-out effect on K_2SO_4. These observations provided a scientific basis for the extraction and separation of K_2SO_4.

Table 5. Solubility of KBr-K_2SO_4-H_2O at 308.15 K and 100.5 kPa [a].

No.	Composition of Liquid Phase/w (%)		Wet Solid Phase/w (%)		Solid Phase
	KBr	K_2SO_4	KBr	K_2SO_4	
1, C_2	0.00	12.05	-	-	Ar
2	3.31	10.25	0.72	81.55	Ar
3	9.57	6.87	2.28	76.11	Ar
4	14.69	4.86	4.70	70.59	Ar
5	18.67	3.69	5.26	72.95	Ar
6	22.70	2.78	7.16	68.92	Ar
7	25.91	2.16	6.54	75.88	Ar
8	29.16	1.79	8.27	72.27	Ar
9	31.99	1.46	10.52	67.72	Ar
10	34.54	1.15	9.76	72.09	Ar
11	37.73	0.85	9.55	75.20	Ar
12	40.29	0.67	8.63	78.81	Ar
13, E_2	41.77	0.59	40.37	20.21	Ar + KBr
14	42.03	0.30	75.17	0.13	KBr
15, D_2	42.21	0.00	-	-	KBr

[a] Standard uncertainties: u(T) = 0.05 K; u(P) = 2 kPa; u(mass fraction) = 0.03; Ar, K_2SO_4.

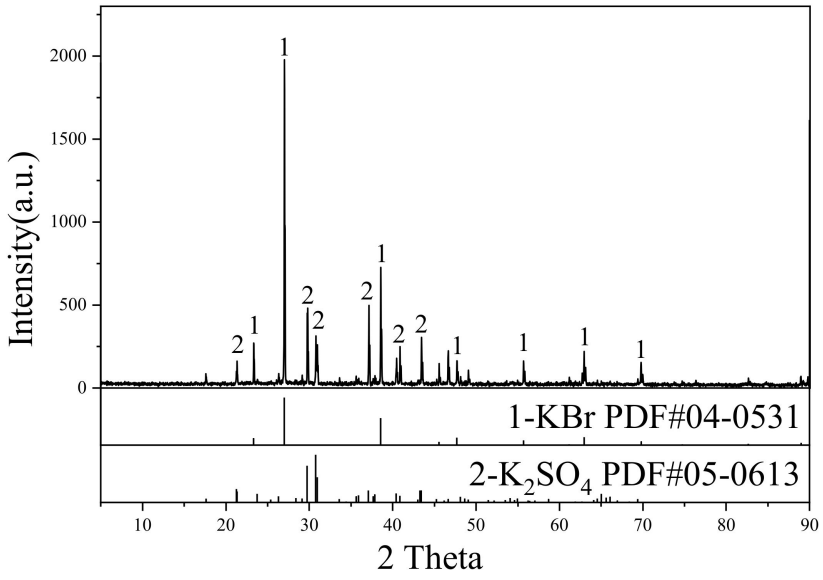

Figure 4. XRD spectrogram of the saturation point E_2 of KBr-K_2SO_4-H_2O at 308.15 K.

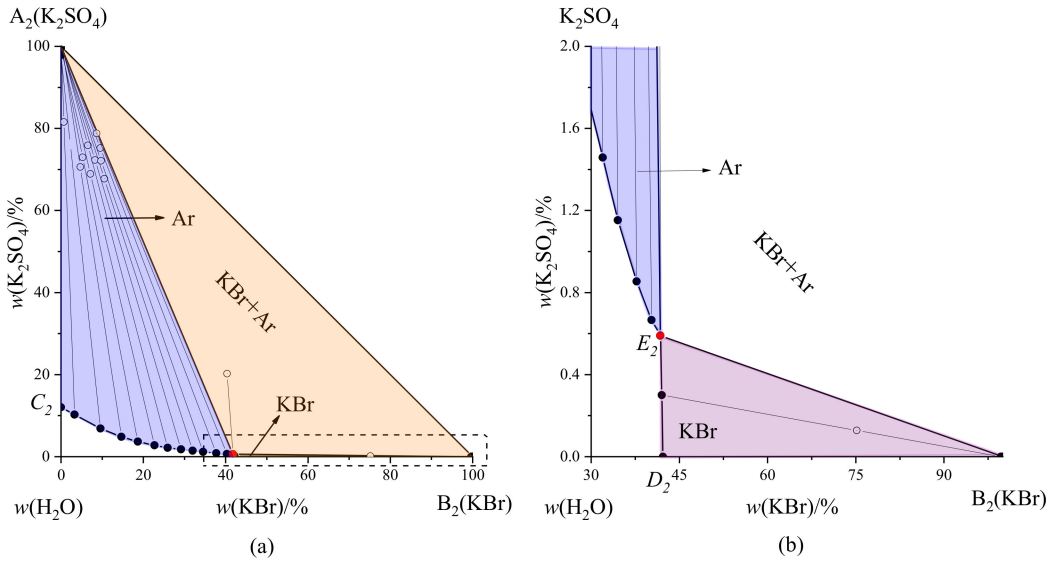

Figure 5. (**a**) Phase diagram of KBr-K_2SO_4-H_2O at 308.15 K and (**b**) enlarged view of point E_2. •, the equilibrium liquid-phase composition point; ○, wet residue composition point.

Table 6. Solid-liquid composition of saturation point. In KBr-K_2SO_4-H_2O system at different temperatures.

Temperature/K	Refs	Composition of Liquid Phase/w (%)		Solid Phase
		KBr	K_2SO_4	
273.15	[18]	34.11	0.00	KBr
		35.54	0.68	KBr + K_2SO_4
		0.00	6.78	K_2SO_4
308.15	this work	42.21	0.00	KBr
		41.77	0.59	KBr + K_2SO_4
		0.00	12.05	K_2SO_4
373.15	[19]	50.98	0.00	KBr
		49.98	0.34	KBr + K_2SO_4
		0.00	19.40	K_2SO_4

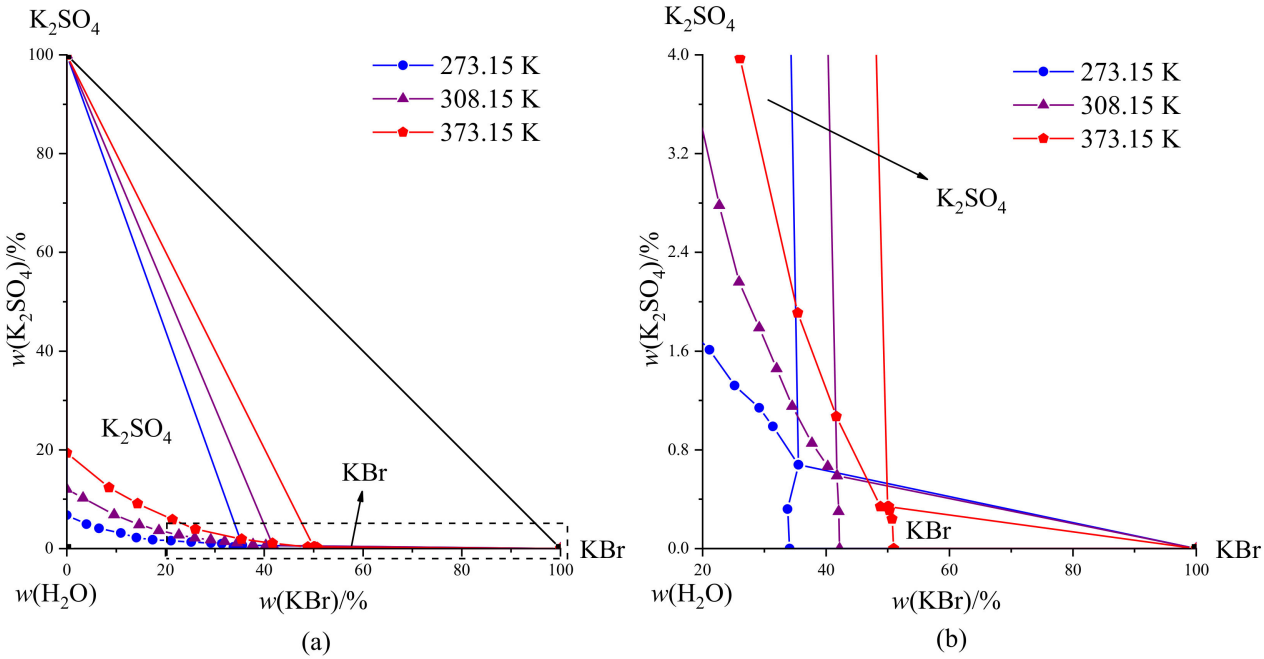

Figure 6. (**a**) Equilibrium phase diagram of ternary system KBr-K_2SO_4-H_2O at different temperatures; (**b**) partial enlargement.

3.3. Phase Equilibrium of the LiBr-Li_2SO_4-KBr-K_2SO_4-H_2O System

Table 7 shows the solubility data of the LiBr-Li_2SO_4-KBr-K_2SO_4-H_2O system at 308.15 K. The XRD characterization results of the solid phase at invariant points E_3, E_4, and E_5 are shown in Figure 7. The dry salt phase diagram of the LiBr-Li_2SO_4-KBr-K_2SO_4-H_2O quaternary system at 308.15 K was plotted according to Table 7, as shown in Figure 8. Points A_3, B_3, C_3, D_3, and F_3 corresponded to the saturation points of each ternary subsystem. The liquid phase composition of each point is presented in Table 7. According to the XRD characterization results, the LiBr-Li_2SO_4-KBr-K_2SO_4-H_2O system contained three saturated points (E_3, E_4, and E_5). The equilibrium solid phases at point E_3 were K_2SO_4, KBr and $K_2SO_4 \cdot Li_2SO_4$, and all ion contents for this composition at this point were $w(K^+)$ = 8.79%, $w(Li^+)$ = 1.04%, $w(Br^-)$ = 28.54%, and $w(SO_4^{2-})$ = 0.87%. The equilibrium solid phases at point E_4 were KBr, $Li_2SO_4 \cdot H_2O$, and $K_2SO_4 \cdot Li_2SO_4$, and all ion contents for this composition were $w(K^+)$ = 0.96%, $w(Li^+)$ = 3.57%, $w(Br^-)$ = 42.91%, and $w(SO_4^{2-})$ = 0.08%. The equilibrium solid phases at point E_5 were $Li_2SO_4 \cdot H_2O$, $LiBr \cdot 2H_2O$, and KBr, and all ion contents for this composition were $w(K^+)$ = 0.74%, $w(Li^+)$ = 5.02%, $w(Br^-)$ = 59.26%, and $w(SO_4^{2-})$ = 0.01%.

Figure 8 shows that there were seven solubility curves, namely, A_3E_3, B_3E_4, C_3E_3, E_3E_4, E_4E_5, D_3E_5, and F_3E_5. The corresponding equilibrium solid phases of A_3E_3 were K_2SO_4 and $K_2SO_4 \cdot Li_2SO_4$, while the corresponding equilibrium solid phases of B_3E_4 were $K_2SO_4 \cdot Li_2SO_4$ and $Li_2SO_4 \cdot H_2O$, those of C_3E_3 were K_2SO_4 and KBr, those of E_3E_4 were $K_2SO_4 \cdot Li_2SO_4$ and KBr, those of E_4E_5 were KBr and $Li_2SO_4 \cdot H_2O$, those of D_3E_5 were $Li_2SO_4 \cdot H_2O$ and $LiBr \cdot 2H_2O$, and those of F_3E_5 were KBr and $LiBr \cdot 2H_2O$. There were five crystallization regions, among which $A_3E_3C_3$, $A_3E_3E_4B_3$, $C_3E_3E_4E_5F_3$, $B_3E_4E_5D_3$, $D_3E_5F_3$ corresponded to the crystalline regions of K_2SO_4, $K_2SO_4 \cdot Li_2SO_4$, KBr, $Li_2SO_4 \cdot H_2O$, and $LiBr \cdot 2H_2O$. The area in each crystalline region was different, and among these, the crystalline region of K_2SO_4 was the largest, accounting for more than 50% of the phase diagram followed by $K_2SO_4 \cdot Li_2SO_4$ double salt, which accounted for about 30–40%, $Li_2SO_4 \cdot H_2O$ and KBr accounted for a few percent, and the crystallization region of $LiBr \cdot 2H_2O$ was very small.

Table 7. Solubility of the LiBr-Li_2SO_4-KBr-K_2SO_4-H_2O system at 308.15 K and 100.5 kPa [a].

No.	Composition of Solution/*w*(%)				Jänecke Index J/(J)			Equilibrium Solid Phases
	Li^+	K^+	Br^-	SO_4^{2-}	$J(Li_2^{2+})$	$J(SO_4^{2-})$	$J(H_2O)$	
1, A_3	1.26	5.31	0.00	15.23	57.16	100.00	2736.54	Ar + Db4
2	1.18	5.15	3.19	12.60	56.44	86.79	2859.03	Ar + Db4
3	1.13	5.09	6.42	10.18	55.48	72.53	2930.61	Ar + Db4
4	1.11	4.92	10.79	7.23	55.93	52.73	2951.30	Ar + Db4
5	1.10	5.37	15.00	5.18	53.56	36.50	2754.78	Ar + Db4
6	1.05	5.62	17.43	3.73	51.37	26.25	2707.28	Ar + Db4
7	1.11	6.66	23.19	1.92	48.37	12.08	2257.28	Ar + Db4
8	1.07	7.51	25.23	1.49	44.61	8.92	2072.09	Ar + Db4
9, E_3	1.04	8.79	28.54	0.87	40.08	4.83	1796.40	Ar + Db4 + Kb
10, C_3	0.00	13.99	28.04	0.33	0.00	1.90	1788.14	Ar + Kb
11	0.14	13.30	28.14	0.42	5.70	2.40	1784.31	Ar + Kb
12	0.35	12.13	28.03	0.48	14.01	2.75	1815.50	Ar + Kb
13	0.46	11.47	27.81	0.57	18.51	3.29	1841.01	Ar + Kb
14	0.67	10.45	28.04	0.64	26.65	3.64	1834.54	Ar + Kb
15	0.80	9.84	28.09	0.72	31.36	4.11	1832.67	Ar + Kb
16	1.43	7.59	30.97	0.57	51.43	2.98	1651.62	Db4 + Kb
17	1.80	6.31	32.78	0.48	61.57	2.37	1548.54	Db4 + Kb
18	2.34	4.14	34.74	0.41	76.10	1.93	1461.26	Db4 + Kb
19	2.76	2.95	37.26	0.32	84.07	1.40	1331.13	Db4 + Kb
20, E_4	3.57	0.96	42.91	0.08	95.44	0.32	1081.07	Db4 + Kb + Ls1
21, B_3	3.20	1.15	0.00	23.57	94.01	100.00	1630.50	Db4 + Ls1
22	2.95	1.11	3.78	19.53	93.77	89.58	1775.88	Db4 + Ls1
23,	2.71	1.06	8.16	15.18	93.54	75.57	1935.24	Db4 + Ls1
24	2.64	1.02	14.18	11.02	93.59	56.38	1940.70	Db4 + Ls1
25	2.50	1.05	16.91	8.39	93.05	45.23	2043.95	Db4 + Ls1
26	2.38	1.03	21.18	4.97	92.84	28.08	2121.04	Db4 + Ls1
27	2.54	1.11	26.36	3.13	92.80	16.47	1878.64	Db4 + Ls1
28	2.84	1.04	34.08	0.46	93.89	2.20	1566.76	Db4 + Ls1
29	3.91	0.91	46.82	0.05	96.04	0.17	913.66	Kb + Ls1
30	5.03	0.82	59.54	0.03	97.18	0.09	514.64	Kb + Ls1
31, E_5	5.02	0.74	59.26	0.01	97.46	0.03	523.25	Kb + Ls1 + Lb2
32, F_3	5.01	0.70	59.05	0.00	97.58	0.00	529.25	Kb + Lb2
33, D_3	5.05	0.00	58.14	0.01	100.00	0.03	561.16	Ls1 + Lb2
34	4.68	0.46	54.77	0.01	98.78	0.03	558.94	Ls1 + Lb2

[a] Standard uncertainties: u(T) = 0.05 K; u(P) = 2 kPa; u(mass fraction) = 0.03; Ar, K_2SO_4; Db4, $K_2SO_4 \cdot Li_2SO_4$; Kb, KBr; Ls1, $Li_2SO_4 \cdot H_2O$; Lb2, $LiBr \cdot 2H_2O$.

Figure 9 shows the water diagram of this quaternary system plotted with $J(2Li^+)$ and $J(H_2O)$. The solubility curve C_3E_3 corresponding to K_2SO_4 and KBr shows smooth fluctuations, indicating that the addition of Li_2SO_4 had a weak effect on the equilibrium. In the solubility curves A_3E_3, B_3E_4, and E_4E_5, the value of $J(H_2O)$ varied greatly with $J(2Li^+)$, indicating that Br^--containing salts had a great influence on the phase equilibrium of this system. The values of $J(H_2O)$ near invariant points E_4 and E_5 were substantially lower than the other parts, suggesting that the mass percentage of H_2O in the solution near the crystallization region of $LiBr \cdot 2H_2O$ was the smallest. A comprehensive analysis of the system shows that K_2SO_4 crystals most readily precipitated from the system, followed by $K_2SO_4 \cdot Li_2SO_4$ double salt crystals, and the $LiBr \cdot 2H_2O$ crystals had the most difficulty precipitating from the system. Bromide salts had a strong salting-out effect on sulfate.

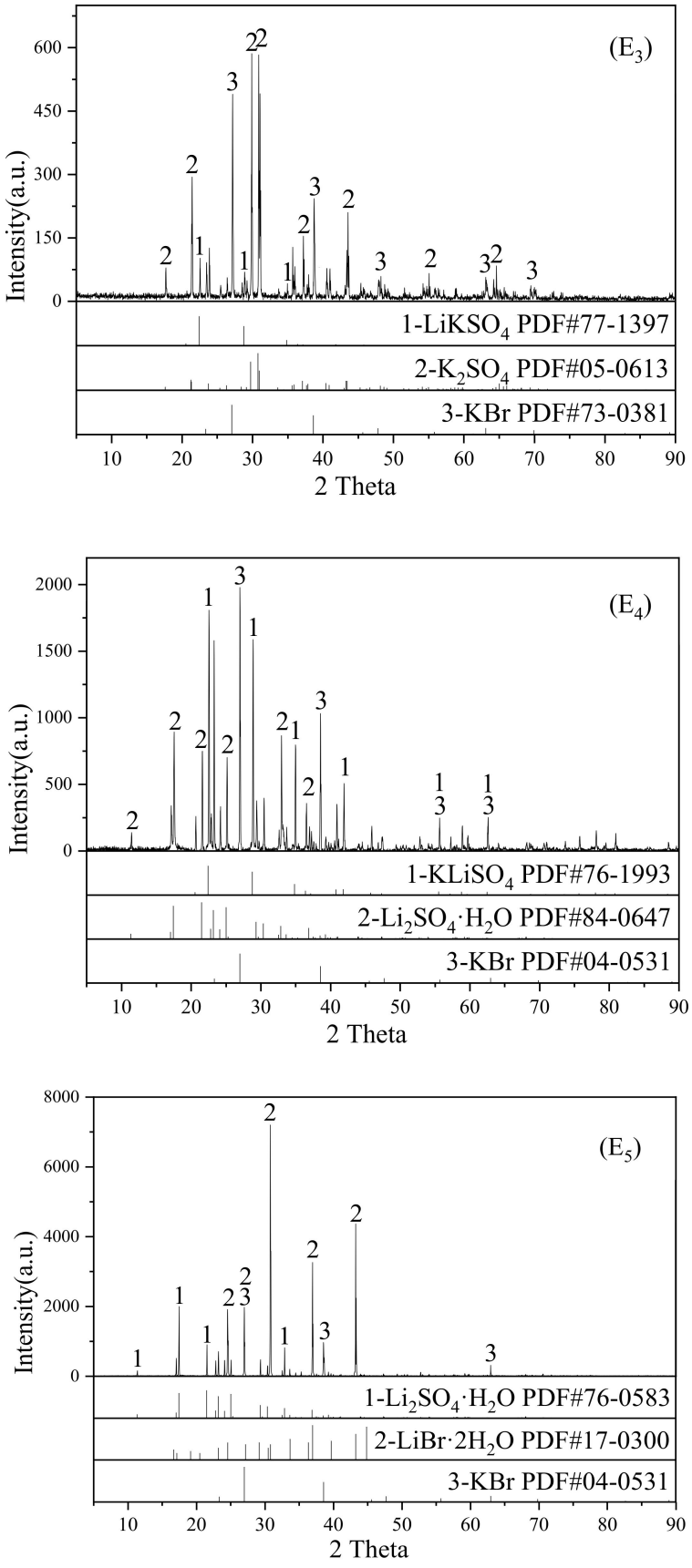

Figure 7. XRD spectrogram of the saturation point E_3, E_4, and E_5 of LiBr-Li_2SO_4-KBr-K_2SO_4-H_2O at 308.15 K.

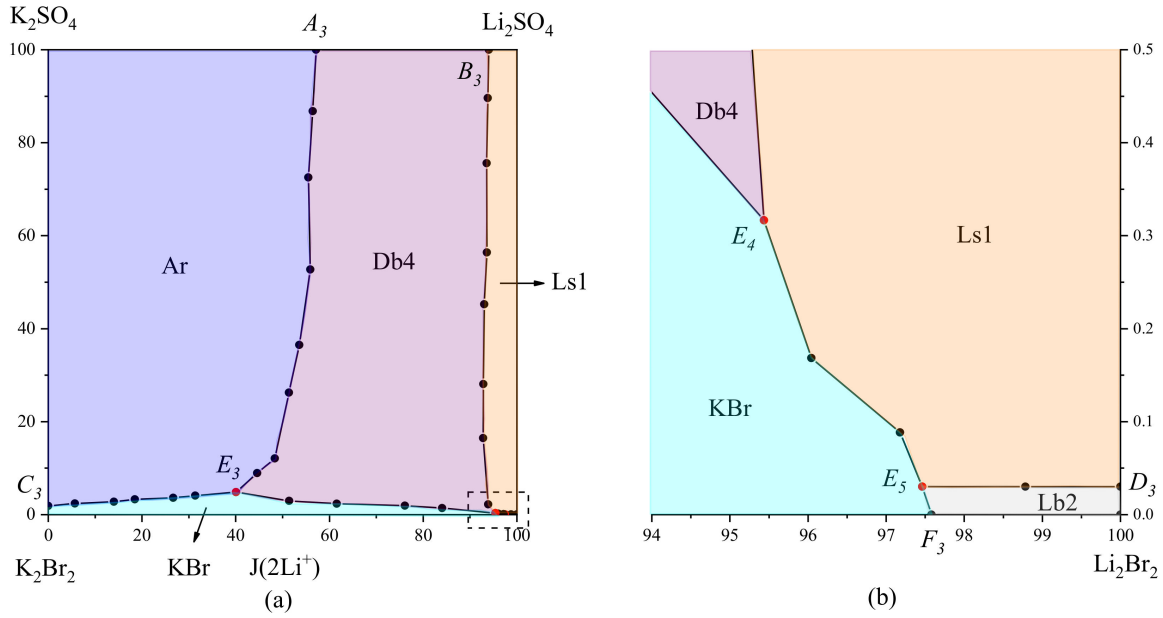

Figure 8. (**a**) Dry salt phase diagram of LiBr-Li_2SO_4-KBr-K_2SO_4-H_2O quaternary system at 308.15 K and (**b**) enlarged view of saturation points E_4 and E_5.

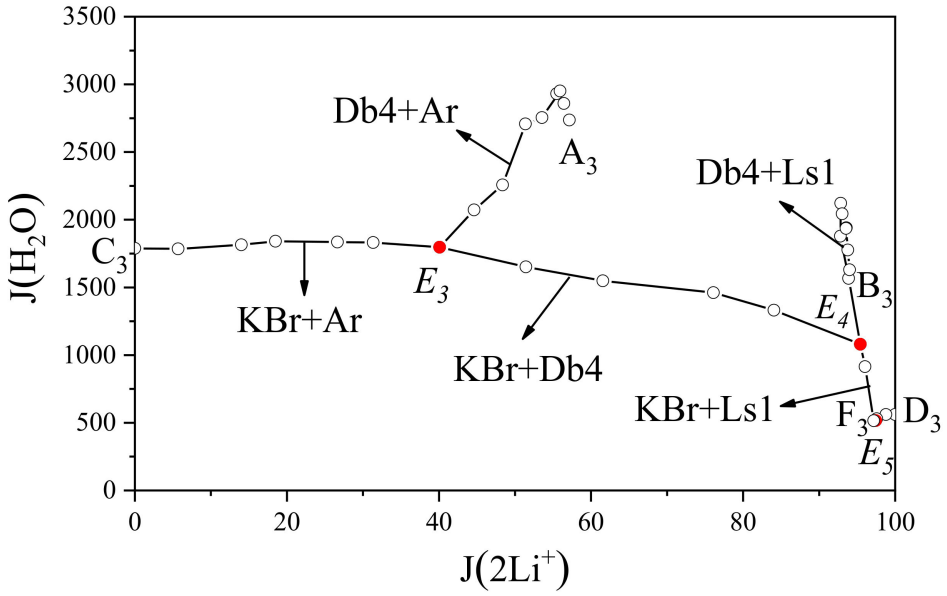

Figure 9. Water content diagram of system LiBr-Li_2SO_4-KBr-K_2SO_4-H_2O at 308.15 K.

By summarizing the phase diagrams of the related systems, we found that double salts occurred in sulfate-containing systems that also contained two of the three elements of lithium, sodium, and potassium [21–27], for example, $K_2SO_4 \cdot Li_2SO_4$, $Na_2SO_4 \cdot Li_2SO_4$, and $Na_2SO_4 \cdot 3K_2SO_4$. After comparing the phase diagrams of the systems, we found that the region of the double salt was relatively large, indicating that the double salt had weak solubility and could be easily separated from the system. However, the salts formed by Cl^-, Br^-, as well as alkali metals and their hydrated salts, which exhibited strong solubility in the system, were difficult to separate from the system.

4. Conclusions

The phase equilibria of quaternary systems (LiBr-Li_2SO_4-KBr-K_2SO_4-H_2O) and their subsystems (LiBr-Li_2SO_4-H_2O, KBr-K_2SO_4-H_2O) were studied. The results showed that at

308.15 K, two hydrated salts ($Li_2SO_4 \cdot H_2O$ and $LiBr \cdot 2H_2O$) formed in the LiBr-Li_2SO_4-H_2O system. The crystallization region of LiBr in this system was considerably smaller than Li_2SO_4, and LiBr had a strong salting-out effect on Li_2SO_4. Compared with the phase equilibrium data of 298.15 K, we found that $LiBr \cdot 2H_2O$ could be precipitated by decreasing the temperature. At 308.15 K, the solid solution and compound salt were not found in the KBr-K_2SO_4-H_2O system, which belonged to a simple co-saturation phase diagram. In addition, the crystallization region of KBr in this system was smaller than K_2SO_4, and KBr had a strong salting-out effect on K_2SO_4. At 308.15 K, the phase diagram of the LiBr-Li_2SO_4-KBr-K_2SO_4-H_2O system consisted of three invariant points, seven solubility curves, and five crystallization regions, i.e., the K_2SO_4, KBr, $Li_2SO_4 \cdot H_2O$, $LiBr \cdot 2H_2O$, and $K_2SO_4 \cdot Li_2SO_4$ crystallization regions. In this system, the crystallization region of $LiBr \cdot 2H_2O$ was the smallest, while K_2SO_4 was the largest, indicating that K_2SO_4 could easily be separated from the system, and this result could be used for the separation and extraction of lithium salts in brine.

Author Contributions: Conceptualization, B.L. and X.J.; methodology, B.L.; validation, B.L., X.J. and J.Y.; investigation, B.L. and X.J.; resources, J.Y.; data curation, B.L.; writing—original draft preparation, B.L. and X.J.; writing—review and editing, B.L., X.J. and J.Y.; supervision, J.Y.; project administration, J.Y. All authors have read and agreed to the published version of the manuscript.

Funding: This research was funded by the National Key Research and Development Programe of China (2016YFB0600504).

Conflicts of Interest: The authors declare no conflict of interest.

References

1. Liu, G.; Zhao, Z.; Ghahreman, A. Novel approaches for lithium extraction from salt-lake brines: A review. *Hydrometallurgy* **2019**, *187*, 81–100. [CrossRef]
2. Zhong, C.F.; Liu, J.; Lv, B.; Ren, D.M. Demand analysis and policy suggestions of Lithium resources in China's new energy vehicle industry. *Energy China* **2018**, *40*, 12–15.
3. Su, T.; Guo, M.; Liu, Z.; Li, Q. Comprehensive Review of Global Lithium Resources. *J. Salt Lake* **2019**, *27*, 104–111.
4. Sun, J.; Dong, Y.; Kong, C. Manufacture of sodium-free lithium chloride from salt lake brine. *Sep. Purif. Technol.* **2014**, *136*, 309–313. [CrossRef]
5. Hu, S.; Sun, Y.; Pu, M.; Yun, R.; Xiang, X. Determination of boundary conditions for highly efficient separation of magnesium and lithium from salt lake brine by reaction-coupled separation technology. *Sep. Purif. Technol.* **2019**, *229*, 115813. [CrossRef]
6. Lin, Y.T.; Chen, S.L. Explorationand Development Prospect of Underground Brinein Sichuan Basin. *J. Salt Lake* **2008**, *16*, 1–7.
7. Zhong, J.; Lin, S.; Yu, J. Li^+ adsorption performance and mechanism using lithium/aluminum layered double hydroxides in low grade brines. *Desalination* **2021**, *505*, 114983. [CrossRef]
8. Zhang, J.; Shi, X.W.; Zhao, S.L.; Song, X.F.; Yu, J.G. Progress in study on phase equilibria of salt-water systems. *Ciesc J.* **2016**, *67*, 379–389.
9. Ye, C.; Wu, Z.Z.; Sang, S.H.; Qi, X.Y.; Liu, X. Solid–Liquid Phase EquiLiBria of Ternary System KBr-LiBr-H_2O at 273.15 K and 308.15 K. *J. Chem. Eng. Data* **2019**, *64*, 5288–5294. [CrossRef]
10. Qi, X.Y.; He, C.X.; Sang, S.H.; Liu, J.; Gao, Y.Y. Solid–liquid equilibria in the quaternary system LiBr-NaBr-KBr-H_2O and its two ternary subsystems at 288.15 K. *Asia-Pac. J. Chem. Eng.* **2021**, *16*, 2595. [CrossRef]
11. Cui, R.Z.; Li, W.; Dong, Y.P.; Li, J. Phase EquiLiBrium and Phase Diagram for the Quaternary System LiBr-NaBr-KBr-H_2O at 298.15 K. *J. Chem. Eng. Data* **2020**, *65*, 3021–3028. [CrossRef]
12. Pelsha, A.D. *Experimental Data on Solubility of Multi-Component Water-Salt Systems*; Chemistry Press: Leningrad, Russia, 1973.
13. Lin, X.F.; Zeng, Y.; Zheng, Z.Y.; Sang, S.H. Study on the metastable diag ram of Li^+, K^+ /SO_4^{2-}-H_2O at 273 K. *Chem. Miner. Process.* **2007**, *36*, 4–6.
14. Bu, B.; Li, L.; Zhang, N.; Guo, Y.; Wang, S.; Sun, L.; Deng, T. Solid–liquid metastable phase equilibria for the ternary system Li_2SO_4-K_2SO_4-H_2O at 288.15 and 323.15 K. *Fluid Phase EquiLiBria* **2015**, *402*, 78–82. [CrossRef]
15. Li, B.; Li, J.; Fang, C.; Wang, Q.Z.; Song, P.S. Study on phase diagrams and properties of solutions in ternary systems Li^+, $K^+(Mg^{2+})/SO_4^{2-}$-H_2O at 25 °C. *Chin. J. Chem.* **1995**, *13*, 112–117. [CrossRef]
16. Li, L.; Bu, B.H.; Zhang, N.; Guo, Y.; Deng, T. Metastable Phase EquiLiBria of the Aqueous Ternary System (Li2SO4-K2SO4-H2O) at 308.15 K. In Proceedings of the 17th National Conference on Chemical Thermodynamics and Thermal Analysis, HangZhou, China, 17–19 October 2014; Chinese Chemical Society: Beijing, China, 2014; pp. 286–287.
17. Zhang, X.P.; Zhou, X.L.; Fan, S.Q.; Wang, Z.; Zheng, H.; Xu, M.Q. Phase equilibria in ternary system LiBr-Li_2SO_4-H_2O at 298 K. *Chem. Eng.* **2020**, *48*, 59–61.
18. Stephen, H.; Stephen, T. *Solubilities of Inorganic and Organic Compounds*; Pergamon Press Macmillan: Oxford, UK, 1979.

19. Lu, Q.F.; Sang, S.H.; Zhang, H.; Li, T. Research of phase equilibria in ternary system KBr-K_2SO_4-H_2O at 373 K. *Inorg. Chem. Ind.* **2015**, *47*, 13–15.
20. Wang, P.; Sang, S.H.; Liu, Q.; Cui, R.Z. Phase EquiLiBria of NaBr-Na_2SO_4-H_2O and KBr-K_2SO_4-H_2O Ternary Systems at 398 K. *J. Chem. Eng. Chin. Univ.* **2016**, *30*, 527–531.
21. Cui, R.Z.; Zhang, Y.M.; Dong, Y.P. Solid-Liquid equilibria of two quaternary systems LiBr-NaBr-Li_2SO_4-Na_2SO_4-H_2O and LiBr-KBr-Li_2SO_4-K_2SO_4-H_2O at 298.15 K. *J. Chem. Thermodyn.* **2022**, *165*, 106665. [CrossRef]
22. Peng, Y.; Zeng, Y.; Su, S. Metastable Phase EquiLiBrium and Solution Properties of the Quaternary System Li^+, K^+/Cl^-, SO_4^{2-}-H_2O at 273.15 K. *J. Chem. Eng. Data* **2011**, *56*, 458–463. [CrossRef]
23. Liu, Y.; Deng, T.; Song, P. Metastable Phase EquiLiBrium of the Reciprocal Quaternary System $LiCl^+KCl^+Li_2SO_4{}^+K_2SO_4{}^+H_2O$ at 308.15 K. *J. Chem. Eng. Data* **2011**, *56*, 1139–1147. [CrossRef]
24. Cui, R.Z.; Yang, L.; Zhang, T.T.; Zhang, X.P.; Sang, S.H. Measurements and calculations of solid–liquid equilibria in the quaternary system NaBr-KBr-Na_2SO_4-K_2SO_4-H_2O at 298.15 K. *Calphad* **2016**, *54*, 117–124. [CrossRef]
25. Sang, S.H.; Sun, M.L.; Li, H.; Zhang, X.; Zhang, K.J. A Study on Equilibria of the Quaternary System Na^+, K^+/Br^-, $SO_4{}^{2-}$-H_2O at 323 K. *Chin. J. Inorg. Chem.* **2011**, *27*, 845–849.
26. Cui, R.Z.; Sang, S.H. Phase equilibria in quaternary system Na^+,K^+/Br^-,$SO_4{}^{2-}$-H_2O at 373 K. *Ciesc J.* **2016**, *67*, 1123–1128.
27. Shen, W.; Ren, Y.; Ma, H.; Mu, H.; Tian, H.; Tang, G. Investigation of Solid–Liquid EquiLiBria on the System Na^+, K^+/Cl^-, $SO_4{}^{2-}$-H_2O and Na^+, $K^+/SO_4{}^{2-}$-H_2O at 313.15 K. *J. Chem. Eng. Data* **2016**, *61*, 2027–2039. [CrossRef]